

DECLARATION

I hereby declare that the thesis entitled "**Self-Assembly of Structurally Diverse Phosphomolybdates: Synthesis, Structure and Properties**", submitted to the University of Calicut in partial fulfillment of the requirements for the award of the Degree of Doctor of Philosophy in Chemistry is a bonafide research work done by me under the supervision and guidance of Dr. Jency Thomas, Assistant Professor, Research & PG Department of Chemistry, St. Thomas College (Autonomous), Thrissur, Kerala.

I further declare that this thesis has not previously formed the basis of any degree, diploma or any other similar title.



Jisha Joseph

ACKNOWLEDGEMENT

*“There’s nothing more calming in difficult moments that knowing there’s someone fighting with you”
- Mother Teresa*

I bow before the Almighty God with a grateful heart, who gave me an opportunity to strive in the path of attaining knowledge. I acknowledge His abiding love and care that has accompanied me throughout this endeavour.

*With profound respect, I accord my deep sentiments of gratitude towards my guide and mentor, **Dr. Jency Thomas**, Assistant Professor, Research & PG Department of Chemistry, St. Thomas College (Autonomous), Thrissur, for her great insights and scholarly advice in providing me with valuable suggestions during the conduct of this study.*

*I express my sincere gratitude towards **Archbishop Mar Andrews Thazhath**, Patron, **Mar Tony Neelankavil**, Manager, **Mar Raphael Thattil**, former Manager, **Very Rev. Fr. Varghese Kuthur**, Executive Manager and **Rev. Dr. Martin Kolambrath**, Bursar, St. Thomas College (Autonomous), Thrissur, for their words of encouragements and blessings.*

*I am indebted to **Dr. Joy K. L.**, Principal, **Dr. Ignatius Antony** and **Dr. Jenson P. O.**, former principals, for their motivation and valuable suggestions.*

*I extend my indebtedness to **Dr. Joby Thomas K.**, HoD, Research & PG Department of Chemistry, St. Thomas College (Autonomous), Thrissur. He was a constant motivator and a powerful visionary in my journey of research work.*

*With deep sense of gratitude I acknowledge the encouragement and insightful comments provided by the faculty members, **Dr. Paulson Mathew**, **Dr. Sunil Jose T.**, **Dr. Jinish Antony M.**, **Ms. Reeja Johnson**, **Dr. Joseph Joly V. L.** and **Mr. Aji C. V.**, Department of Chemistry, St. Thomas College (Autonomous), Thrissur. I thank the office staff and non-teaching staff for their kind support.*

*This effort couldn’t be completed without the cooperation and support of our research group members, **Memsy C. K.** and **Raji C. R.** I extend my sincere thanks to the research scholars in the Department of Chemistry, St. Thomas (Autonomous), Thrissur particularly **Dinoop Lal S**, **Drishya Sasidharan**, **Binsi M. Paulson**, **Ragi K.**, **Anju Rose Puthukkara P.**, **Swathy T. S.**, **Rohini Das K.**, **Nithya C. S.**, **Neera Rajan M.** and **Akhila N. S.** for their cooperation and timely support.*

*I am grateful to **Prof. A. Ramanan** at Department of Chemistry, Indian Institute of Technology, Delhi for allowing me to visit his lab during April-May 2019. I thank **Dr. Balendra Kumar**, **Bharti Singh** and **Manisha Jadon** for all the help during the two months spent at IIT Delhi.*

I also thank DST- FIST and UGC-CPE sponsored Infrared & UV-Visible spectrometer and PXRD facilities at our college. I am grateful to Sophisticated Test and Instrumentation Centre (STIC), Cochin University for providing instrumentation facilities. I am thankful to CH Muhammed Koya library at University of Calicut for the plagiarism check.

*I gratefully place on record my deep sentiments of respect to my provincial superior **Rev. Dr. Jasmine Maria CMC**, former provincials **Rev. Sr. Jeesa CMC**, **Rev. Sr. Bency CMC**, **Rev. Sr. Mary James CMC** and provincial councillors for giving me the permission to pursue research and for their countless blessings and immense inspiration.*

I also remember with grateful heart my friends and well-wishers. Without their tremendous understanding and constant encouragement it would be impossible for me to complete my study.

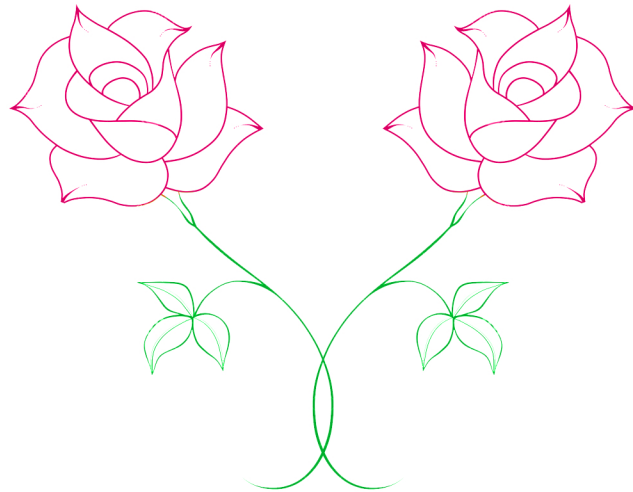
*I cannot but be thankful to my community members – **Mrs. Mary Jolly Kattookaren**, **Sr. Sophy Ans CMC**, **Sr. Ann Julia CMC**, **Sr. Mary Varghese CMC** and **Sr. Jiya Anns CMC** for their great support and encouragement throughout my research.*

*Words are no measure to describe the forbearance and fortitude with which my family has encouraged me. My Parents **Joseph K. V.** and **Elsy Joseph**, and my sisters **Jeeja Binoy** and **Jyothy Sajesh** have they made my dream come true, through their valuable prayers and silent sacrifices.*

Jisha Joseph

Dedicated to,

**SACRED HEART CMC PROVINCE
MANANTHAVADY**



*As we express our gratitude,
we must never forget that
the highest appreciation is not
words, but to live by them.*

John F Kennedy

PREFACE

Phosphomolybdate (PMO) is an important sub-class of Polyoxometalates (POMs). This phosphorous and molybdenum containing heteropolyanions comprise of a distinguished family with versatile structural features and promising applications. The counter cations of these anionic clusters can be metal ions, metal complexes or protonated organic moieties. The Phosphomolybdates are widely classified into various types. Among these, Strandberg-type $\{P_2Mo_5O_{23}\}^{6-}$, Keggin-type $\{PMo_{12}O_{40}\}^{3-}$, Wells Dawson-type $\{P_2Mo_{18}O_{62}\}^{6-}$ and as fully reduced cluster $\{P_4Mo_6O_{31}\}^{12-}$ are the predominant types. Since they are supramolecular materials they can self-assemble into tuneable size and shape with varying dimensionality. In this thesis, seven novel Strandberg-type PMOs and one copper based Keggin-type solid have been reported along with their characterization and related physico-chemical properties. Ammonium Phosphomolybdate (APM) which is a Keggin-type PMO was synthesized along with its two composites with polyaniline and poly (N-methylaniline), namely APM/PAni and APM/PNMAAni respectively. APM was found to be a good ion-exchanger to remove cationic dye-stuffs from its aqueous solution with high efficiency and appreciable reusability. The Cr(VI) removal efficiency of APM and its composites have been investigated and APM/PNMAAni was observed as a good candidate for the same.

Two synthetic methods have been used in the thesis namely, solvent evaporation technique and hydrothermal technique. In the first method, P and Mo precursors along with organic moiety and metal chlorides were taken in the form of clear aqueous solution and kept undisturbed for the self-assembly process. The slow evaporation of the solution at room temperature resulted in crystallization of PMO based solids. In the second method, a hydrothermal bomb was used; which is a sealed Teflon container. The reaction

was carried out under autogenous pressure and the precursors were added along with water. A temperature range from 100-180°C was selected for a time span of 3 days. The slow cooling of the apparatus was allowed for the crystallization of solids.

The thesis is divided into seven chapters. Chapter I comprises of a brief introduction to the work, giving emphasis to the synthetic routes, different classes of PMOs based on their structural features and properties along with their important applications. A literature survey on the research carried out in this area for the past decade was carried out and systematically tabulated.

In chapter II, two new Strandberg cluster (referred to as $\{P_2Mo_5\}$) based PMOs namely, $\{H-2a3mp\}_5[\{PO_3(OH)\}\{PO_4\}Mo_5O_{15}]$, and $\{H-2a4mp\}_5[\{PO_3(OH)\}\{PO_4\}Mo_5O_{15}] \cdot 6H_2O$ were synthesized *via* solvent evaporation technique using 2-amino-3-methylpyridine (*2a3mp*) and 2-amino-4-methylpyridine (*2a4mp*) respectively. These solids formed a supramolecular framework stabilized by hydrogen bonding interaction between cluster anions and organic moieties. CH... π interactions between the organic moieties reinforced the crystal packing. The electrochemical behaviour of the synthesized solids was explored by means of three electrode system using 1 mM $K_4[Fe(CN)_6]$ in 0.1 M KCl as supporting electrolyte. In addition, the optical band gaps of the solids were also calculated using ultraviolet-diffused reflectance spectroscopy data. Cyclic voltammogram of both the solids showed reversible waves corresponding to Mo^{VI}/Mo^V electron process. The optical band gap energies of the solids showed slight difference on account of their difference in the nature of the ligands.

In chapter III, self-assembly of molybdate and phosphate precursors in the presence of zinc ions and organic ligands *viz.* benzimidazole (*bimi*), 4-aminopyridine (*4-ap*) and pyrazole (*pz*), has been carried out under hydrothermal condition. The crystallization of

Strandberg cluster based solids $\{Hbimi\}_5[HP_2Mo_5O_{23}].5H_2O$, $\{Hbimi\}_6[P_2Mo_5O_{23}].H_2O$, $\{4-Hap\}_4[H_2P_2Mo_5O_{23}].2H_2O$, $\{4-Hap\}_5[HP_2Mo_5O_{23}]$ and $\{Hpz\}_6\{Zn(pz)_4(H_2O)_2\}[\{Zn(pz)_2P_2Mo_5O_{23}\}_2].8H_2O$ was observed. The chapter highlights the structural differences in the supramolecular isomers; and the effect of supramolecular isomerism and nature of ligands on the optical band gap energies (E_g) of the synthesized solids.

In chapter IV, an attempt was made to crystallize phosphorous and molybdenum precursors in the presence of $MCl_2.xH_2O$ ($M = Co, Ni, Cu$ and Zn) with pyrazole to form PMO solids of varying dimensionality. The solids obtained were: $\{Hpz\}_6\{Zn(pz)_4(H_2O)_2\}[\{Zn(pz)_2P_2Mo_5O_{23}\}_2].8H_2O$, $[\{Cu(pz)_4\}_2\{H_2P_2Mo_5O_{23}\}].H_2O$, $\{Ni(pz)_4\}[\{Ni(pz)_4\}_2\{H_2P_2Mo_5O_{23}\}_2] [\{Ni(pz)_4\}\{Ni(pz)_4(H_2O)\}\{HP_2Mo_5O_{23}\}_2].14H_2O$, $[Ni(pz)_4Cl_2]$, $\{pz\}_2[\{Co(pz)_4\}_5\{P_2Mo_5O_{23}\}_2].6H_2O$ and $[\{Cu(pz)_2\}_4\{CuMo_{12}O_{38}(OH)_2\}].8H_2O$. Among these, the last solid is a rare example of copper based Keggin cluster. Except for this solid, which was synthesized using hydrothermal method; all other solids were obtained via solvent evaporation method. The magnetic properties of the solids were investigated using Guoy Balance.

In chapter V, synthesis, characterization and dye removal efficiency of ammonium phosphomolybdate (APM) which is a Keggin-type solid has been discussed. It was concluded that APM could be effectively used as an ion-exchanger to remove cationic dye-stuffs from aqueous solution. The dyes used for investigation were methylene blue, malachite green, methyl red and eosin. The influence of parameters such as nature of light, amount of APM, contact time and pH on dye removal efficiency was investigated.

In chapter VI, the synthesis and characterization of two composites of APM with polyaniline and poly (N-methylaniline), namely APM/PAni and APM/PNMA ni respectively have been summarised. The difference in band gap energy in APM upon the

formation of the composite was investigated, and the capacity of these composites in the removal of hexavalent chromium from aqueous solution was explored. It was concluded that APM/PNMA_{ni} could effectively reduce harmful Cr(VI) to environmentally benign Cr(III).

Chapter VII concludes the entire work and emphasizes the future scopes of PMO based hybrid solids.

LIST OF ABBREVIATIONS

1. APM	Ammonium phosphomolybdate
2. APM/PAni	Ammonium phosphomolybdate/polyaniline composite
3. APM/PNMAAni	Ammonium phosphomolybdate/poly(N-methylaniline) composite
4. APS	Ammonium persulphate
5. BET	Brunauer-Emmett-Teller
6. BVS	Bond valence sum
7. CTAB	Cetyl trimethyl ammonium bromide
8. CV	Cyclic voltammetry
9. DDW	Double distilled water
10. DMF	Dimethyl formamide
11. DMSO	Dimethyl sulphoxide
12. DPC	Diphenyl carbazide
13. EDAX	Energy dispersive X-ray spectroscopy
14. EY	Eosin
15. FESEM	Field emission scanning electron microscope
16. FTIR	Fourier Transform Infrared
17. GCE	Glassy carbon electrode
18. JCPDS	Joint committee on powder diffraction standards
19. MB	Methylene blue
20. MG	Malachite green
21. MR	Methyl red

22. ORTEP	Oak ridge thermal ellipsoid plot
23. PAN	Polyacrylonitrile
24. PAni	Polyaniline
25. PMA	Phosphomolybdic acid
26. PMMA	Polymethylmethacrylate
27. PMO	Phosphomolybdate
28. PNMAAni	Poly(N-methylaniline)
29. {P ₂ Mo ₅ }	{P ₂ Mo ₅ O ₂₃ } ⁶⁻
30. {PMo ₁₂ }	{PMo ₁₂ O ₄₀ } ³⁻
31. {P ₄ Mo ₆ }	{P ₄ Mo ₆ O ₃₁ } ¹²⁻
32. POM	Polyoxometalates
33. PXRD	Powder X-ray diffraction
34. rGO	Reduced graphene oxide
35. SEM	Scanning electron microscopy
36. TGA	Thermogravimetric analysis
37. TMC	Transition metal complex
38. UV-DRS	Ultraviolet-Diffused reflectance spectroscopy
39. UV-Vis	Ultraviolet-visible
40. <i>2a3mp</i>	2-amino-3-methylpyridine
41. <i>2a4mp</i>	2-amino-4-methylpyridine
42. <i>bimi</i>	Benzimidazole
43. <i>4-ap</i>	4-aminopyridine
44. <i>pz</i>	Pyrazole

45. 0-D	Zero dimensional
46. 1-D	One dimensional
47. 2-D	Two dimensional
48. 3-D	Three dimensional

ABSTRACT

Polyoxometalate (POM) is an important class of early transition metal-oxygen clusters with plentiful intrinsic structures and widespread applications. Phosphomolybdate (PMO), a prominent sub-class of POMs, has been attracting the attention of researchers on account of their versatile building blocks and controllable architectures. Supramolecular self-assembly is a powerful tool to create PMO solids with attracting properties. Important factors affecting the self-assembly process are nature of organic moiety, temperature, pH of the medium and nature of metal ions. Owing to the controllable external factors, the self-assembly can lead to the formation of supramolecular aggregates with varying size and dimensionality such as one dimensional chain, two dimensional sheets and three dimensional networks. Moreover, nitrogen donor ligands and their pH related nature play a vital role in the crystal engineering. They have the capability to form complex with metal centres or undergo protonation. Recently a new trend of designing composite materials of PMOs with suitable substances like polymers has been observed.

In this thesis, various novel PMOs with varying structure and dimensionality have been synthesized. The characterization of the synthesized solids was done successfully by single crystal X-ray diffraction, powder X-ray diffraction, fourier transform infrared spectroscopy and thermo gravimetric analysis. The behavior and dynamics of these solids on account of their non-bonding interactions involved in the self-assembly process and affecting factors have been illustrated. Some predominant properties of the synthesized solids like optical band gap energy, magnetic properties and electrochemical properties were investigated. Ammonium phosphomolybdate (APM), a member of Keggin-type PMO was synthesized and characterized. Its ability to remove cationic dye-stuffs from aqueous solutions was explored. Two unique composites of APM with

polyaniline and poly(N-methylaniline) *viz.* APM/PAni and APM/PNMAAni were synthesized and characterized. Moreover, APM/PNMAAni composite was found as a good candidate to reduce environmental pollutant Cr(VI) to Cr(III) from contaminated aqueous solution.

TABLE OF CONTENT

CONTENTS		Page No.
List of Tables		xix
List of Figures		xxi
List of Schemes		xxix
Chapter I	Introduction and Review of Literature	1-39
	Summary.....	1
I.1	Introduction	2
I.2	Types of PMO clusters.....	4
I.2.1	Strandberg-type cluster $\{P_2Mo_5O_{23}\}^{6-}$	4
I.2.2	Keggin-type cluster $\{PMo_{12}O_{40}\}^{3-}$	5
I.2.3	Wells Dawson-type cluster $\{P_2Mo_{18}O_{62}\}^{6-}$	6
I.2.4	Fully reduced cluster $\{P_4Mo_6O_{31}\}^{12-}$	7
I.3	Classification of PMO cluster based solids	9
I.3.1	Class I	9
I.3.2	Class II	14
I.3.3	Class III	16
I.3.4	Class IV	19
I.4	Structural features in PMO cluster based solids	21
I.4.1	Supramolecular isomerism	21
I.4.2	Aggregation of water clusters	22
I.4.3	Porosity	23
I.5	Synthetic strategies	24
I.5.1	Solvent evaporation technique	24
I.5.2	Hydrothermal synthesis	25
I.6	Applications of PMOs	25
I.6.1	Biomedical applications	25
I.6.2	Applications in catalysis	27
I.6.3	Applications in magnetism	29
I.6.4	Electrochemical applications.....	30
I.7	Motivation for the present study.....	31

References	33
------------------	----

Chapter II	Role of supramolecular interactions in crystal packing of Strandberg-type cluster based hybrid solids	41-67
-------------------	--	--------------

	Summary.....	41
II.1	Introduction	42
II.2	Experimental Section	43
II.2.1	Synthesis.....	43
II.2.2	Characterization	44
II.2.2.1	X-ray crystallographic studies.....	44
II.2.2.2	Powder X-ray diffraction (PXRD).....	44
II.2.2.3	Fourier transform infrared (FTIR) spectroscopy.....	45
II.2.2.4	Thermogravimetric analysis (TGA)	46
II.2.2.5	Scanning electron microscopy (SEM).....	46
II.2.2.6	Cyclic voltammetric studies.....	46
II.2.2.7	Band gap energy calculations.....	46
II.3	Results and Discussion.....	47
II.3.1	Crystal structure of 1 and 2	47
II.3.2	Analysis of solids 1 and 2	54
II.3.3	Electrochemical behavior.....	59
II.3.4	Band gap energy calculations.....	60
II.3.5	Chemistry of Formation.....	63
II.4	Conclusions.....	64
	References.....	65

Chapter III	Supramolecular isomerism in {P₂Mo₅} cluster based solids	69-111
--------------------	---	---------------

	Summary.....	69
III.1	Introduction.....	70
III.2	Experimental Section.....	71
III.2.1	Synthesis.....	71
III.2.2	Characterization.....	72

III.3	Results and Discussion.....	72
III.3.1	Crystal structure of 3	74
III.3.2	Crystal structure of 4	77
III.3.3	Crystal structure of 5 and 6	82
III.3.4	Analysis of solids 3-6	93
III.3.5	Band gap energy calculations.....	101
III.3.5.1	Effect of ligands on band gap energy.....	101
III.3.5.2	Effect of protonation on band gap energy.....	104
III.3.6	Chemistry of Formation.....	106
III.4	Conclusions.....	108
	References	110
Chapter IV	Metal pyrazole complex incorporated PMO cluster based solids	113-143
	Summary.....	113
IV.1	Introduction.....	114
IV.2.	Experimental Section.....	119
IV.2.1	Synthesis.....	119
IV.2.1.1	Solvent evaporation method.....	119
IV.2.1.2	Hydrothermal synthesis.....	120
IV.2.2	Characterization.....	121
IV.2.3	Magnetic susceptibility measurements.....	122
IV.3	Results and discussion.....	122
IV.3.1	Crystal structure of 7	122
IV.3.2	Crystal structure of 8	124
IV.3.3	Crystal structure of 9	124
IV.3.4	Crystal structure of 10	126
IV.3.5	Crystal structure of 11	127
IV.3.6	Crystal structure of 12	128
IV.3.7	Analysis of solids 7 and 12	131
IV.4	Magnetic properties.....	139
IV.5	Conclusions.....	140

	References.....	142
Chapter V	Removal of cationic dyes from water using APM	145-172
	Summary.....	145
V.1	Introduction	146
V.2	Experimental Section.....	150
V.2.1	Synthesis of APM.....	150
V.2.2	Synthesis of dye solutions	150
V.2.3	Treatment of dye-contaminated water.....	150
V.3	Characterization.....	151
V.4	Results and discussion.....	152
V.4.1	Characterization of APM particles.....	152
V.4.2	Treatment of dye contaminated water.....	154
V.4.2.1	Effect of nature of light.....	154
V.4.2.2	Effect of contact time.....	157
V.4.2.3	Effect of amount of APM.....	158
V.4.2.4	Effect of nature of dye.....	159
V.4.2.5	Influence of pH.....	161
V.4.2.6	Reusability of APM.....	161
V.4.2.7	Adsorption capacity of APM.....	163
V.4.2.8	Mechanism.....	164
V.5	Conclusions.....	168
	References.....	169
Chapter VI	Investigations using composites based on APM	173-200
	Summary.....	173
VI.1	Introduction	174
VI.2	Experimental Section.....	178
VI.2.1	Synthesis of APM/Polymer composite.....	178
VI.2.2	Synthesis of polymers.....	178
VI.3	Characterization.....	179
VI.4	Results and discussion	179
VI.4.1	Characterization of APM/PAni.....	179

VI.4.2	Characterization of APM/PNMA _{ni}	180
VI.5	Electrochemical behavior of composites.....	183
VI.6	Optical band gap energy (E_g) determination applying Kubelk- a–Munk (KeM or F(R)) function in Tauc method	185
VI.7	Removal of Cr(VI) from aqueous solution.....	189
VI.7.1	Procedure for Cr(VI) removal.....	190
VI.7.2	Cr(VI) removal studies using the components of composites.....	190
VI.7.3	Effect of amount of PNMA _{ni}	191
VI.7.4	Effect of contact time.....	192
VI.7.5	Cr(VI) removal using APM/PNMA _{ni}	193
VI.7.6	Proposed mechanism for Cr(VI) removal	194
VI.8	Conclusions	197
	References.....	198
Chapter VII	Summary and Conclusion	201-202

Publications and Conference presentations

LIST OF TABLES

Table No.	TITLE OF TABLE	Page No.
CHAPTER I: INTRODUCTION		
I.1	Class I solids wherein PMO clusters are covalently linked to TMCs extending into multi-dimensions	11
I.2	Class II solids having discrete PMO clusters with TMCs as counter cations	15
I.3	Class III solids in which PMO clusters derivatized by TMCs	17
I.4	Class IV solids having coordination polymers incorporating PMOs	20
CHAPTER II: ROLE OF SUPRAMOLECULAR INTERACTIONS IN CRYSTAL PACKING OF STRANDBERG-TYPE CLUSTER BASED HYBRID SOLIDS		
II.1	Crystallographic details for 1 and 2	45
II.2	Hydrogen bonding interactions in 1	48
II.3	Hydrogen bonding interactions in 2	51
II.4	O...O interactions in 2	54
II.5	Table tabulates the irrespective, allowed indirect and allowed direct band gaps of 1 and 2	62
CHAPTER III: SUPRAMOLECULAR ISOMERISM IN {P₂MO₅} CLUSTER BASED SOLIDS		
III.1	Crystal and Refinement Data for Solids 4-6a	73
III.2	H-bonding interactions in 3	74
III.3	H-bonding interactions in water tetrameric unit of 3	76
III.4	H-bonding interactions in 4	81
III.5	CH... π interactions in 4	81
III.6	H-bonding interactions in 5	83
III.7	O...O interactions in 5	85
III.8	H-bonding interactions in 6a	88
III.9	CH... π and π ... π interactions in 6a	88
III.10	H-bonding interactions in 6b	91
III.11	Table tabulates the irrespective, allowed indirect and allowed direct band gaps of 1 , 2 , 3 and 6a	103

III.12	Table tabulates the irrespective, allowed indirect and allowed direct band gaps of 5 , 6a and 6b	104
III.13	Ligands and their pK _a values	107
CHAPTER IV: METAL PYRAZOLE COMPLEX INCORPORATED PMO CLUSTER BASED SOLIDS		
IV.1	Table summarizing pyrazole incorporated TMC in PMO cluster based solids reported in literature during the past decade	115
IV.2	Classification of Solids 7-11	117
IV.3	Crystal and Refinement Data for Solids 7 , 9 and 12	121
IV.4	BVS calculations of 12	129
IV.5	The summary of thermal degradation analysis of 7 , 9 and 10	139
CHAPTER V: REMOVAL OF CATIONIC DYES FROM WATER USING APM		
V.1	Table summarizing the results obtained using APM for degradation of dye-stuffs	148
V.2	Absorbance of MB solution upon treatment with APM at 660 nm after 1 hour of irradiation under different conditions	155
V.3	Absorbance of MB solution upon treatment with APM at 660 nm upon varying time of contact	158
V.4	Absorbance of MB solution upon treatment with APM at 660 nm after each cycle	163
V.5	Textural parameters of APM before (I) and after (II) the treatment of dye-stuffs	164
CHAPTER VI: INVESTIGATIONS USING COMPOSITES BASED ON APM		
VI.1	A preview of PMO ₁₂ based composites reported in the past decade	175
VI.2	Weight % of elements present in APM/PAni from EDAX	182
VI.3	Weight % of elements present in APM/PNMAAni composite	182
VI.3	Table tabulates the irrespective, allowed indirect and allowed direct band gaps of APM, APM/PAni and APM/PNMAAni	188

LIST OF FIGURES

Figure No.	TITLE OF FIGURE	Page No.
CHAPTER I: INTRODUCTION		
I.1	(a) Ball-and-stick (b) polyhedral view of Strandberg-type anion	6
I.2	(a) Ball-and-stick (b) polyhedral view of α -Keggin anion	6
I.3	(a) Ball-and-stick (b) polyhedral view of Wells Dawson-type anion	8
I.4	(a) Ball-and-stick representation of top view of basic structural unit of $\{P_4Mo_6O_{31}\}^{12-}$ (b) polyhedral view of $\{P_4Mo_6O_{31}\}^{12-}$. (c) Side view and (d) top view of hourglass-type $\{M(P_4Mo_6O_{31})_2\}$	8
I.5	(a) Figure showing coordination of $\{P_2Mo_5O_{23}\}^{6-}$ cluster anion with Cu(1) and Cu(2). (b) 1-D chain in $[H_3O]_2[Cu_2(Pyim)_2(H_2O)_3][P_2Mo_5O_{23}].6H_2O$	10
I.6	Ball-and-stick and polyhedral representation of $[Cu(L)_2(H_2O)_2]_2H_2[P_2Mo_5O_{23}].2CH_3OH$ ($L =$ pyridine-2-carboxamide)	15
I.7	1-D chain of $Mg[Cu(bim)(H_2O)]_2[P_2Mo_5O_{23}].4H_2O$ which depicts the linkage of Mg^{2+} ion through the oxygen atoms of the $\{P_2Mo_5\}$ cluster anion	17
I.8	1-D chain formed in $[Cu_3(4,4'\text{-bis(pyrazol-1-ylmethyl)biphenyl})_3][PMo_{12}O_{40}]$	20
I.9	Supramolecular isomerism exhibited by $(imi)(Himi)_2[\{Cu(imi)_2\}_2H_2P_2Mo_5O_{23}]$	23
I.10	Decameric water cluster in $(Himi)_3[\{Cu(imi)_3(H_2O)_2\} \{HP_2Mo_5O_{23}\}].3H_2O$	23
I.11	$\{PMo_{12}\}$ clusters are linked by ammonium ions through H-bonding interaction to form porous 2-D sheet in ammonium phosphomolybdate	24
CHAPTER II: ROLE OF SUPRAMOLECULAR INTERACTIONS IN CRYSTAL PACKING OF STRANDBERG-TYPE CLUSTER BASED HYBRID SOLIDS		
II.1	An ORTEP view of (a) 1 and (b) 2	48
II.2	(a) 1-D chains in 1 mediated by O...O interactions between terminal oxygen atoms O22 and O23 of phosphate groups of neighboring cluster anions. Formation of 1-D chains is also facilitated by CH...O interactions mediated by $\{N1N2\}$ moieties. (b) H-bonding interactions	49

	exhibited by $\{HP_2Mo_5\}$ cluster anion in 1 . (c) Formation of zig-zag 2-D sheet through CH...O and $\pi... \pi$ interactions between neighboring 1-D chains	
II.3	(a) CH... π and $\pi... \pi$ interactions form a octameric unit. (b) Crystal packing in 1 is facilitated by CH... π interactions between neighboring sheets. (c) CPK representation of 1 showing solvent accessible voids	50
II.4	(a) Dimeric unit in 2 wherein $\{HP_2Mo_5\}$ cluster anions are linked through H-bonding mediated by $\{N7N8\}$ moiety. The pentameric water cluster is anchored to the dimer through O...O interactions. (b) The pentameric water cluster in 2 . (c) Dimer units linked through water clusters to form 1-D chain propagating along <i>b</i> axis. The 1-D chains result in voids which are occupied by $\{N9N10\}$ moieties	52
II.5	(a) The connection between chains through H-bonding interaction (N6H6B...O16: 2.127(5) Å) and CH... π interactions to form a sheet. (b) CH... π interactions in 2 . (c) Neighboring 2-D sheets are further linked by lattice water molecule, O1W to form a 3-D supramolecular network	53
II.6	FTIR Spectra of (a) 1 and (b) 2	55
II.7	SEM images of (a) 1 and (b) 2	55
II.8	TGA curve of 1 and 2	56
II.9	Simulated and Experimental PXRD of 1	57
II.10	Simulated and Experimental PXRD of 2	58
II.11	(a) Cyclic voltammogram for 1 and 2 in the presence of 1 mM $K_4[Fe(CN)_6]$ in 0.1 M KCl with a scan rate of 50 mVs ⁻¹ (b) Comparison of voltammogram of <i>2a4mp</i> with bare GCE and solid 2	60
II.12	Plots of (a) Reflectance versus wavelength (b) F(R) versus $h\nu$ (eV), (c) $(F(R)h\nu)^{1/2}$ versus $h\nu$ (eV) and (d) $(F(R)h\nu)^2$ versus $h\nu$ (eV) for 1	61
II.13	Plots of (a) Reflectance versus wavelength (b) F(R) versus $h\nu$ (eV), (c) $(F(R)h\nu)^{1/2}$ versus $h\nu$ (eV) and (d) $(F(R)h\nu)^2$ versus $h\nu$ (eV) for 2	62
CHAPTER III: SUPRAMOLECULAR ISOMERISM IN $\{P_2MO_5\}$ CLUSTER BASED SOLIDS		
III.1	(a) $\{HP_2Mo_5\}$ anion shows extensive H-bonding interaction with the five (<i>Hbimi</i>) ⁺ moieties. (b) The dimeric units are connected by $\{N1N3\}$ moiety to form ladder-like 1-D chains propagating along <i>a</i> axis. (c)	75

	View along <i>a</i> axis showing the connection between one 1-D chain with six others. (d) H-bonding interactions exhibited by lattice water molecules	
III.2	(a) $\pi \dots \pi$ interactions between {N10N12} and {N13N15} moieties. (b) CH... π and $\pi \dots \pi$ interactions between {N1N3}, {N4N6} and {N7N9} moieties forming a hexameric unit	76
III.3	(a) ORTEP view of 4 . (b) 1-D chains formed via H-bonding interactions mediated by protonated {N5N6} moieties. (c) NH...O interactions mediated by {N7N8} moiety link neighboring 1-D chains to form a 2-D corrugated sheet. (d) View along <i>a</i> axis showing the crystal packing of 2-D corrugated sheets	78
III.4	(a) While three of the (<i>Hbimi</i>) ⁺ moieties viz. {N5N6}, {N7N8} and {N9N10} are linked to each other through CH... π interactions; {N3N4} and {N11N12} merely form a dimer as seen in (b). (c) The H-bonding in 1-D chains of 4 is reinforced through CH... π interactions	79
III.5	The packing of 1-D chains is also facilitated through CH... π interactions. CH... π interactions mediated by {N7N8} moieties favors the crystal packing in 4	80
III.6	ORTEP view of (a) 5 and (b) 6a	83
III.7	(a) NH...O interactions mediated by {N1N2} and {N5N6} moiety link {H ₂ P ₂ Mo ₅ } cluster anions to form 2-D sheet through N-H...O interactions (2.069(3)-2.208(3) Å). The third (<i>Hampy</i>) ⁺ moiety viz. {N7N8} is encapsulated in the voids of 2-D sheet through N-H...O interaction (2.286(4) Å). (b) View along <i>b</i> axis	85
III.8	(a) Figure showing packing of sheets. Two of the sheets are connected via H-bonding interactions mediated by {N1N2} and lattice water molecule, O1W. The voids formed as a result of crystal packing of 2-D sheets are occupied by {N3N4} moieties and lattice water molecule, O2W shown in brown and pink color respectively. (b) CH... π interactions between {N5N6}, {N3N4} and {N1N2}	85
III.9	(a) H-bonding interactions between (4- <i>Hap</i>) ⁺ moieties and {P ₂ Mo ₅ } cluster anions forming 1-D zig-zag chains in 6a . (b) View along <i>b</i> -axis	86
III.10	(a) The 1-D chains are connected through H-bonding interactions	87

	mediated by {N5N6} moieties to form 2-D corrugated sheet having voids. (b) Figure showing 2-D corrugated sheet having voids are occupied by {N1N2} moieties CH... π and π ... π interactions between {N1N2} and {N3N4} moieties form a tetrameric unit. (c) Three of the 2-D corrugated sheets. Each sheet exhibits H-bonding interactions with neighbouring sheets through {N1N2} moieties accommodated in its voids. The tetramers are connected through CH... π interactions mediated by {N5N6} moieties belonging to neighboring 2-D corrugated sheets	
III.11	(a) CH... π and π ... π interactions between {N1N2} and {N3N4} moieties form a tetrameric unit. (b) The tetramers are connected through CH... π interactions mediated by {N5N6} moieties	89
III.12	(a) Figure showing the formation of dimeric unit in 6b . (b) Each of the dimeric units is connected via H-bonding interactions to form 1-D chains	90
III.13	Figure showing two 1-D chains connected via H-bonding mediated by {N9N10} moieties. The inter-chain voids are occupied by {N3N4} units	91
III.14	(a) The {N3N4} units in inter-chain voids are part of interpenetrating 2-D sheets perpendicular to sheet shown in Figure III.13. The lattice water molecules along with {N3N4} units act as nodes connecting the interpenetrating sheets. Inter-sheet spaces are occupied by {N1N2} and {N5N6} moieties (π ... π : 3.550 Å) which are anchored to lattice water molecule O5W. (b) Figure showing the two sets of interpenetrating sheets	93
III.15	FTIR spectrum of (a) 3 and (b) 4	94
III.16	FTIR spectrum of (a) 5 and (b) 6a	94
III.17	Simulated and Experimental PXRD of 3	95
III.18	Simulated and Experimental PXRD of 4	96
III.19	Simulated and Experimental PXRD of 5	97
III.20	Simulated and Experimental PXRD of 6a	98
III.21	Simulated and Experimental PXRD of 6b	99
III.22	TGA of 4 , 5 and 6a	100
III.23	Plots of (a) Reflectance versus wavelength (b) F(R) versus $h\nu$ (eV), (c)	102

	(F(R)hν) ^{1/2} versus hν(eV) and (d) (F(R)hν) ² versus hν(eV) for 3	
III.24	Plots of (a) Reflectance versus wavelength (b) F(R) versus hν(eV), (c) (F(R)hν) ^{1/2} versus hν(eV) and (d) (F(R)hν) ² versus hν(eV) for 6a	103
III.25	Plots of (a) Reflectance versus wavelength (b) F(R) versus hν(eV), (c) (F(R)hν) ^{1/2} versus hν(eV) and (d) (F(R)hν) ² versus hν(eV) for 5	105
III.26	Plots of (a) Reflectance versus wavelength (b) F(R) versus hν(eV), (c) (F(R)hν) ^{1/2} versus hν(eV) and (d) (F(R)hν) ² versus hν(eV) for 6b	106
CHAPTER IV: METAL PYRAZOLE COMPLEX INCORPORATED PMO CLUSTER BASED SOLIDS		
IV.1	Statistical analysis of TMC incorporated PMO cluster based solids reported in literature during the last two decades	118
IV.2	(a) Transition metal substituted Keggin type polyanion by replacing the central atom and (b) transition metal substituted Keggin type phosphomolybdate by replacing one of the addenda atoms	119
IV.3	1-D chains in 7	123
IV.4	(a) Octahedral {Zn(pz) ₄ (H ₂ O) ₂ } ²⁺ complex links 1-D chains along with six (Hpz) ⁺ cations to form 2-D sheets (H-bonding interactions are shown in dashed red lines). (b) View along <i>a</i> axis	123
IV.5	3-D crystal packing is facilitated by CH...π interaction between neighboring sheets	124
IV.6	Zig-zag chains in 8 connected by Cu1 to form 3-D structure of 8	125
IV.7	(a) Asymmetric unit in 9 . (b) Tetrameric cluster unit forming 2-D sheet as shown in (c)	126
IV.8	Six coordinated nickel complex of [Ni(pz) ₄ Cl ₂], 10	127
IV.9	(a) Co1 and Co2 complex units covalently link {P ₂ Mo ₅ } clusters into 2-D sheets. (b) Co3 complex units connect the sheets to form a double sheet	128
IV.10	Keggin type polyanion which contains copper as the central atom. Two protonated terminal oxygen atoms (O6) are shown in cyan	130
IV.11	2-D sheet formed connecting polyanions via copper- pyrazole complexes	130
IV.12	The hexameric water cluster in which the O...O interactions shown in solid red lines	131

IV.13	FTIR of (a) 7 and (b) 8	132
IV.14	FTIR of (a) 9 and (b) 10	132
IV.15	FTIR of (a) 11 and (b) 12	132
IV.16	Simulated and Experimental PXRD of 7	133
IV.17	Simulated and Experimental PXRD of 8	134
IV.18	Simulated and Experimental PXRD of 9	135
IV.19	Simulated and Experimental PXRD of 10	136
IV.20	Simulated and Experimental PXRD of 11	137
IV.21	Simulated and Experimental PXRD of 12	138
IV.22	TGA of 7, 9 and 10	139
CHAPTER V: REMOVAL OF CATIONIC DYES FROM WATER USING APM		
V.1	(a) Indexed PXRD pattern (b) FTIR spectrum (c) SEM image and (d) TGA curve of as-synthesized APM particles	154
V.2	UV-Vs spectra of (i) original solution of Methylene Blue (MB) having pH = 5.0±0.1 and (ii) MB solution obtained after treatment with APM followed by exposure to dark, sun light or UV for 1 hour. Figures in the inset represent the original solution of MB (Bottle A) and filtrate of Bottle A obtained after treatment with APM followed by exposure to dark, sun light or UV for 1 hour (Bottle B-D) respectively	156
V.3	The PXRD pattern of APM before (a) and after treatment with MB solution collected from (b) Bottle B (c) Bottle C and (d) Bottle D	156
V.4	Figure in the inset shows the results obtained for time bound decolourization of MB (pH = 5.0±0.1). (i) Original dye solution (ii) Dye solution immediately after adding APM. (iii)-(vii) Filtrate collected after 0, 15, 30, 45 and 60 minutes respectively (a) and (b) Represent the corresponding UV-Visible spectra of original MB solution i.e. Bottle (i) and filtrate of Bottles (iii-vii) respectively	157
V.5	Figure showing the decrease in intensity of absorbance peak of MB solution ($\lambda_{\max} = 660 \text{ nm}$) upon increasing the amount of APM	159
V.6	UV-Visible spectra of 25 mL of 10^{-5} M dye solution having pH = 5.0±0.1 of (a) MB (b) MG (c) MR and (d) EY before (coloured curve) and after (black curve) treatment with 0.125 g of APM. Figure in the inset shows (i) original dye solution (ii) dye solution immediately after	160

	adding 0.125 g of APM (iii) filtrate of Bottle ii immediately after 5 minutes of stirring	
V.7	(a) and (b) Dye solutions of MR at pH above and below 5 respectively with (i) original dye solution (ii) dye solution immediately after adding 0.125 g of APM (iii) filtrate of bottle (ii) immediately after 5 minutes of stirring. (c) and (d) UV-Visible spectra of dye solutions (i) and (iii) of MR shown in Figure 7a and 7b respectively.(e) and (f) Structure of MR at pH above and below 5 respectively	162
V.8	The adsorption/desorption isotherm of APM which resembles that of Brunauer's Type I isotherm	164
V.9	(a) Crystal structure of APM. The lattice water molecules have been omitted for clarity. (b) Ion-exchange between NH_4^+ ions and cationic dye moieties	165
V.10	Figure showing the PXRD pattern of (a) as-synthesized APM (b) APM obtained after 1 st cycle of treatment with MB solution (c) APM obtained after 16 th cycle of treatment with MB solution	166
V.11	Release of ion-exchanged dye moieties in solution upon treatment with 1M NH_4Cl and NH_3 solution. (a) Ion-exchange mechanism for MR. (b) Ion-exchange mechanism for MB and MG	167
CHAPTER VI: INVESTIGATIONS USING COMPOSITES BASED ON APM		
VI.1	(a) FTIR spectrum of APM/PAni composite (b) PXRD pattern of (i) APM (ii) APM/PAni-composite (iii) PAni (c) SEM image and (d) EDAX spectrum of APM/PAni-composite	181
VI.2	(a) FTIR spectrum of APM/PNMAAni (b) PXRD pattern of (i) APM (ii) PNMAAni and (iii) APM/PNMAAni-composite (c) SEM image and (d) EDAX of APM/PNMAAni-composite	183
VI.3	(a) CV of bare GCE and APM coated on GCE. (b) CV of APM/PAni and APM/PNMAAni coated on GCE	184
VI.4	Plots of (a) Reflectance versus wavelength (b) $F(R)$ versus $h\nu(\text{eV})$, (c) $(F(R)h\nu)^{1/2}$ versus $h\nu(\text{eV})$ and (d) $(F(R)h\nu)^2$ versus $h\nu(\text{eV})$ for APM	186
VI.5	Plots of (a) Reflectance versus wavelength (b) $F(R)$ versus $h\nu(\text{eV})$, (c) $(F(R)h\nu)^{1/2}$ versus $h\nu(\text{eV})$ and (d) $(F(R)h\nu)^2$ versus $h\nu(\text{eV})$ for APM/PAni	187

VI.6	Plots of (a) Reflectance versus wavelength (b) F(R) versus $h\nu$ (eV), (c) $(F(R)h\nu)^{1/2}$ versus $h\nu$ (eV) and (d) $(F(R)h\nu)^2$ versus $h\nu$ (eV) for APM/PNMAAni composite	188
VI.7	The UV-Vis spectra for Cr(VI) removal by PANi, PNMAAni and APM; along with 2 ppm Cr(VI) solution	191
VI.8	The UV-Vis spectra for Cr(VI) removal by PNMAAni with varying amount	192
VI.9	The UV-Vis spectra for Cr(VI) removal by PNMAAni at different time intervals	193
VI.10	The UV-Vis spectra for original Cr(VI) solution and for the solution obtained after adding APM/PNMAAni at $\text{pH} = 1-5 \pm 0.5$	194
VI.11	UV-Vis spectra of (a) ammonium heptamolybdate solution and (b) filtrate collected during composite formation after stirring one hour	197

LIST OF SCHEMES

Scheme No.	TITLE OF SCHEME	Page No.
I.1	Scheme showing a few examples of isopolyanions and heteropolyanions of molybdenum	3
III.1	Scheme showing the experimental procedure to crystallize solids 3-7	72
IV.1	Scheme showing the experimental procedure to crystallize solids 7-11	120
VI.1	Procedure for the synthesis of APM/PAni and APM/PNMAAni	178
VI.2	The scheme for the removal of Cr(VI) using poly(N-methylaniline)	195
VI.3	Scheme showing the mechanism for reduction of Cr(VI) to Cr(III) using APM/PNMAAni composite	196